Geothermal Mineralization I: The Mechanism of Formation of the Beowawe, Nevada Siliceous Sinter Deposit

by

J. D. Rimstidt
Department of Geological Sciences
Virginia Polytechnic Institute and State University

and

David R. Cole
Earth Science Laboratory
University of Utah Research Institute

January 1982

Prepared for
U.S. Department of Energy
Division of Geothermal Energy
Work Performed Under Contract DE-AC07-80ID12079
submitted for publication in The American Journal of Science

NOTICE

This report was prepared to document work sponsored by the United States Government. Neither the United States nor its agent, the United States Department of Energy, nor any Federal employees, nor any of their contractors, subcontractors or their employees, makes any warranty, express or implied, or assumes any legal liability or responsibility for the accuracy, completeness, or usefulness of any information, apparatus, product or process disclosed, or represents that its use would not infringe privately owned rights.

NOTICE

Reference to a company or product name does not imply approval or recommendation of the product by the University of Utah Research Institute or the U.S. Department of Energy to the exclusion of others that may be suitable.

GEOTHERMAL MINERALIZATION I: The Mechanism of Formation of the Beowawe, Nevada Siliceous Sinter Deposit

J. D. Rimstidt
Department of Geological Sciences
Virginia Polytechnic Institute and State University
Blacksburg, VA 24061

David R. Cole
Earth Sciences Laboratory
University of Utah Research Institute
Salt Lake City, UT 84108

ABSTRACT. The siliceous sinter deposit at Beowawe, Nevada has a volume of 7.71×10^7 m^3 and contains 1.28×10^{11} kg silica. This silica precipitated from geothermal solutions that welled-up along the Malpais Fault, a graben bounding fault. Sinter formation involved three steps: (1) Geothermal solutions that were saturated with quartz in the reservoir moved to the surface where they cooled and became supersaturated with amorphous silica. (2) Amorphous silica particles nucleated (heterogeneously on ferric hydroxides) to produce a colloidal suspension. (3) The amorphous silica particles agglomerated and were cemented together by amorphous silica precicitating in the embayments between the particles. At least 5.58×10^{14} kg of geothermal solution must have been produced over time to account for the mass of silica in the Beowawe Deposit. This fluid would have carried at least 4.95×10^{17} kJ of heat to the surface.

INTRODUCTION

Siliceous sinter deposits are common features of many high temperature geothermal areas. Such areas are often characterized by boiling hot springs and geysers that produce dilute, alkaline waters. Sinter deposits occur as terraces around these features and are composed of predominately white to tan or gray, often banded, friable to dense, vitreous masses of amorphous silica. The formation of siliceous sinter requires that the geothermal solutions contain a high enough silica concentration to become saturated with amorphous silica when they cool through the 100 to 50°C range. The silica concentration of the geothermal solution is controlled by the solubility of quartz under reservoir conditions (Fournier and Rowe, 1966) so that a boiling spring depositing sinter at 100° must be fed by water containing at least 370 ppm dissolved silica. This silica concentration could only be produced in a reservoir that is hotter than 235° (fig. 1).

==========

Figure 1.--near here

==========

For a spring depositing sinter at 50°C the reservoir must be at least 175°C. Thus, siliceous sinter deposits are unlikely to form in geothermal areas where the reservoir temperature is less than 200°C.

In this paper we will describe the features of the large Beowawe, Nevada siliceous sinter deposit and discuss a

general model for its formation. The geology of the Beowawe, Nevada area is described in detail in Struhsacker (1980) and Zoback (1979) and is sumarized here for the conveinence of the reader.

The Beowawe geothermal system, located astride the Lander-Eureka county line in the Whirlwind Valley of north-centeral Nevada (fig. 2) is a hot-water system with measured temperatures ranging from 160°C at 1830 m depth to 212°C at a depth of 2915 m (Ginn 1-13 well).

==========

Figure 2.--near here

==========

Exposed reservoir rocks within the Beowawe area include the Paleozoic siliceous eugeosynclinal rocks of the Valmy Formation and overlying Tertiary volcanic units. The Valmy Formation consists of siliceous siltstone with significant amounts of quartzite, sandstone, bedded chert, siliceous conglomerate, and locally bedded barite. The Tertiary volcanics range in composition from basalt to dacite and include dikes, flows, and tuffs locally interbedded with interflow tuffaceous and alluvial horizons. In general, pervasive alteration through the Miocene volcanic section has produced a smectite-calcite-quartz-hematite assemblage near the surface that grades into a smectite-chlorite-calcite-quartz-pyrite assemblage at depth (Cole, in prep.). Below the Tertiary-Ordivician contact, the rocks are weakly altered to a quartz-calcite-pyrite-chlorite-smectite-epidote

assemblage.

Three major episodes of structural development are recognized within the geothermal area: a Paleozoic thrust faulting event, a northwest-trending graben developed during the mid-Miocene, and northeast-trending Basin and Range faulting. As a result of thrusting, allochthonous siliceous rocks of the Ordivician Valmy Formation lie in exposed fault contact upon the subjacent autochthonous carbonates along the Roberts Moutain Thrust of the upper-Devonian to lower-Mississippian Antler Orogeny (see Zoback, 1979 for schematic sections). At a much later time, major northwest-trending fractures were produced by rifting along the Oregon-Nevada lineament. These confined laterally a thick sequence of middle-Miocene, calc-alkaline to alkaline volcanic flows. The northeast-trending faults that have produced the principle topographic feature in the area, the Malpais Rim, represent the final period of Basin and Range faulting. These normal faults post-date all volcanic units. The sinter terrace has developed along the fault-controlled Malpais Rim which bounds the southeast margin of Whirlwind Valley (fig. 2).

THE BEOWAWE SINTER DEPOSIT

The Beowawe Sinter Deposit is located along the trace of the graben bounding fault that produced the Malpais Rim. This deposit is more than 65 m thick and 1.6 km in length and is estimated to contain more than 1.28×10^{11} kg of silica. Situated on this sinter terrace are numerous hot

springs and fumaroles (fig. 2). Before intensive geothermal exploration disrupted the local hydrology, there were at least three active geysers on the sinter terrace (Nolan and Anderson, 1934 and Rinehart, 1968). Presently most of the hot water production is from uncapped exploration wells and numerous springs. The estimated combined discharge is about 400 liters per minute (Renner, et al., 1975). The temperature of the boiling springs is around 93°C which is the boiling point of water at the 5000 foot elevation of the deposit. Down hole temperature measurements and chemical geothermometers show subsurface temperatures of 200 to 250° with an average temperature of about 230°C being most probable. The geothermal waters are dilute, slightly alkaline, sodium bicarbonate-sulfate solutions (see Nolan and Anderson, 1934 and Table 1 for analyses).

==========

Table 1.--near here

==========

Although the sinter terrace cannot be examined completely from top to bottom, several areas of excellent exposure do exist which can be documented. The most conspicuous feature of the terrace, in addition to its size, is the layering that has resulted from accretion of siliceous material. This layering can be classified into three categories on the basis of scale. On the scale of meters to tens of meters, the sinter has the appearance of a normal sediment, with separate units on the order of tens of

centimeters in thickness. Some of these units are massive with fine-grained siliceous material forming a matrix that encloses larger opaline fragments or shards whose long axes lie parallel to the dip of the unit. Other units have a very fissile almost shale-like texture with an average of two to five parting planes per centimeter. This parting plane phenomena is the second class of layering. Commonly, a very dense opaline unit lies at the contact between either two massive units or a fissile unit and a massive unit. These opaline units are typically pure white but may contain black or gray bands that are only a few millimeters thick. Small solution cavities and channels are common above these dense opaline units. The third type of layering recognizable in the sinter is a millimeter scale banding. In general, each parting plane contains this finest layering but it is often obscured by white siliceous dust. These fine laminations are characteristically tinted red with iron oxide stains in the upper portions of the sinter pile, but they become more opaline or vitreous toward the base of the sinter pile.

The attitudes of the layering are variable depending on the location on the terrace. At the top of the terrace, near the Malpais Rim, dips are relatively low, averaging less than ten degrees to the north, away from the rim. Further down and out into the pile, the units dip from 18° to 20° away from the Malpais Rim. At the bottom of the pile, the units are again nearly flat-lying with dips

averaging less than five degrees and without a prefered orientation.

Bulk density measurements made on seven samples selected from the sinter pile range from 1.33 to 2.12 g cm^{-3}, and have an average of 1.66±0.3 g cm^{-3}. Compared to the density of silica minerals these values indicate that the void space in the sinter may be as high as 50%.

The total mass of siliceous material can be calculated if the volume of the sinter pile is known. A computer graphics technique was used to determine the area within each of the contours on the sinter deposit as shown in figure 2. It was assumed that each sub-area (12 in all) could be approximated by a rectangular block with a base at 4680 elevation. The total volume of the pile was determined by summing the volumes of each of the 12 separate blocks each having a unique area and heigth. This technique yielded a total volume for the pile of 7.71×10^7 m^3 (0.077 km^3). If the average bulk density of the sinter is 1.66 g cm^{-3} as calculated above, the mass of siliceous material in the pile is 1.28×10^{11} kg. This is within an order of magnitude of the value of 1.76×10^{10} kg that was estimated by Zoback (1979).

MECHANISM OF SINTER FORMATION

There are three main steps in siliceous sinter formation. First, geothermal solutions, that have equilibrated with the quartz in the surrounding rocks, move to the surface and become supersaturated with amorphous

silica as they cool. Second, amorphous silica particles nucleate and grow to produce a colloidal suspension. Finally, the suspended amorphous silica particles agglomerate and are cemented together to form sinter.

While the geothermal fluid is in the reservoir, it is equilibrated with the quartz in the surrounding rocks (Fournier and Rowe, 1966). When some of this fluid escapes toward the surface, it travels down a steep thermal gradient so that it rapidly becomes supersaturated with quartz. However, in areas with high discharge rates, the rate of ascension of the fluid toward the surface is generally so fast that there is not time for a significant amount of silica to precipitate from the solution (Rimstidt and Barnes, 1980). At or very near the surface, the solution finally cools to the saturation temperature of amorphous silica. When the geothermal solution is discharged onto the surface amorphous silica precipitation begins.

Quartz is the thermodynamically most stable form of silica under geothermal conditions and according to simple silica-water kinetics it should always precipitate more rapidly than amorphous silica (Rimstidt and Barnes, 1980). However, in sinter deposits the least stable silica polymorph, amorphous silica, precipitates instead. This phenomonon has often been observed in other systems and is known as Ostwald's Step Rule. Ostwald's Step Rule can be stated as: In highly supersaturated systems, the least stable (most soluble) polymorph of the solid often

precipitates rather than the thermodynamically stable one; the metastable precipitate then recrystalizes stepwise to more and more stable polymorphs until equilibrium is achieved. While this is an empirical rule and is not followed by all systems, it seems to hold for many geochemical situations, including silica precipitation from geothermal solutions.

The phenomenon of precipitation of metastable solids is observed when the solution is so supersaturated that nucleation rather than simple molecular deposition dominates the precipitation process. An important factor in nucleation kinetics is the effect of the surface free energy of a particle of very small size on its stability. In general, the free energy of formation of a particle of radius, r, is:

$$\Delta G_f = -\{(4/3)\pi r^3 \Delta G_f^o/V\} + \{(4x10^{-10})\pi r^2 \sigma\}$$

(Uhlmann and Chalmers, 1966). Here, ΔG_f is the free energy of formation of particles of radius, r; ΔG_f^o is the free energy of formation of the bulk solid; V is the molar volume of the solid; σ is the surface free energy of the solid in contact with the aqueous solution. Spherical geometry is assumed in the following discussion for simplicity. The first term is the free energy contribution of the bulk solid and the second is the free energy of formation of the interface between the particle and the aqueous solution. This relationship can be recast in terms of the solubility

of particles of radius, r:

$$\ln (c/c^{\circ}) = \{(2/3)\sigma VB\}/\{rRT\}$$

Here, c is the solubility of particles of radius, r; c° is the solubility of the bulk solid; σ is the surface free energy of the solid in contact with the aqueous solution; V is the molar volume of the solid; B is a geometric factor (16.8 for spheres). The effect of particle size on amorphous silica solubility is illustrated in figure 3.

==========

Figure 3.--near here.

==========

Thus, as a nuclei grows from a single molecule to a particle of macroscopic dimensions its free energy of formation first increases because its surface area is large relative to its volume, and then with further growth the volume term becomes large enough to outweigh the surface area term and the free energy of formation constantly decreases with further growth. This means that the free energy of formation of the particle passes through a maximum where the free energy contribution from the surface is just balanced by the free energy driving the precipitation (fig. 4).

==========

Figure 4.--near here.

==========

Thus, a particle with a radius larger than the critical radius will grow spontaneously. The flux of molecules (J)

onto the growing nuclei as they pass through this process is given by:

$$J = \nu \exp\{B\sigma^3V^2/kT(RT \ln S)^2\}$$

(Nielsen, 1964). ν is a pre-exponential factor (10^{30} has been used here); B is a geometric factor (16.8 for spherical particles); σ is the surface free energy of the solid in contact with the aqueous solution; V is the molar volume of the solid; k is Boltsmans constant; and S is the degree of saturation of the solution. This equation can be evaluated if the surface free energies of quartz and amorphous silica are known. Alexander (1957) has determined the surface free energy of amorphous silica to be about 45 ergs cm^{-2} by measuring the solubility of very small particles. Unfortunately, no direct measurement of the surface free energy of quartz has been made so it must be estimated using a correlation between the surface free energy of a solid and its solubility (Nielsen and Sohnel, 1971). Using 6 ppm as the solubility of quartz yields a surface free energy of about 120 ergs cm^{-2}.

The above data were used with equation 3 to calculate the rates of homogeneous nucleation of quartz and amorphous silica as a solution containing 345 ppm dissolved silica (saturated with quartz at 230°C) cools. The surface free energies of the solids were assumed to be constant over this temperature interval. The results of this calculation are shown in figure 5.

==========

Figure 5.--near here.

==========

A flux of around 10^{-13} moles kg^{-1} sec^{-1} is equivalent to the removal of about ten percent (35 ppm) of the dissolved silica from solution per day. Fluxes lower than this can be considered insignificant in terms of sinter formation, and in fact, considerably higher fluxes are probably responsible for most sinter precipitation. The scales at the top of the diagram show that quartz is always more supersaturated than amorphous silica. However, the rate of quartz precipitation would not become significant until the solution cooled to about 25°C. Near this temperature the rate of amorphous silica precipitation exceeds that of quartz so there is no way for significant amounts of quartz to nucleate. Thus, the only mechanism for precipitation of quartz in geothermal systems it epitaxial growth on already existing quartz grains and it has already been shown that precipitation by this mechanism is slow (Rimstidt and Barnes, 1980).

Two factors indicate that in sinter deposition amorphous silica precipitation is catalyzed by the presence of suspended solids that act as heterogeneous nuclei. First, according to the the results displayed in figure 5, if amorphous silica precipitates by a homogeneous nucleation mechanism a significant amount of silica precipitation would not occur until the geothermal solution has cooled to around 25°C. Second, careful experiments by Makrides, et al.

heterogeneous mechanism can be estimated from equation 3 by replacing the surface free energy of the pure solid with an effective free energy for the composite nuclei. A value of 10 to 20 erg cm^{-2} would explain the scaling rates observed in many geothermal power extraction systems and the temperature range in which most siliceous sinter is formed in the Beowawe system (fig. 5). On the other hand, quartz is a crystalline material whose lattice configuration is not nearly as flexible as amorphous silica so the potential for heterogeneous nucleation of quartz is severly limited. This explains the near absence of primary quartz in most geothermal scale and sinter deposits. Note that when the effective surface free energy is very low the contours of nucleation rate as a function of temperature (fig. 5) are very steep. This means that once the solution cools to the temperature of critical saturation nearly all of the silica nucleates over a temperature interval of less than 5°. Thus, the onset silica deposition is abrupt and is confined to a narrow zone around the vent where the water rapidly cools through this critical temperature interval.

The most important substances that catalyze amorphous silica nucleation are ferric hydroxides. This is born out by observations of the rate of formation of siliceous scales in geothermal energy extraction systems. Experience with silica scaling in the geothermal power extraction systems of the Imperial Valley of California shows that the severity of scaling increases toward the north where both the geothermal

solutions and the scale become more iron rich. Furthermore, scale formation experiments by Rothbaum et al. (1979) using geothermal fluids from Broadlands and Wairakei showed that aeration of the geothermal fluids produced a significant increase in the rate of scale formation as a result of the oxidation of ferrous iron to ferric iron. The ferric iron then precipitates from the neutral to slightly alkaline solutions as amorphous ferric hydroxides. Because ferric hydroxides cannot form in the unaerated solutions that are in the vents and quiet pools, these features do not become filled and choked by sinter deposition, but rather, most of the sinter deposits occur on the flanks of these features where the flowing water is both aerated, to produce ferric hydroxide nuclei, and cooled rapidly through the critical temperature range.

The final step in the formation of siliceous sinter is the agglomeration and attachment of the suspended particles to the surface of the sinter deposit. This process is effected by the direct precipitation of dissolved silica into the contact zone between two silica particles. Silica precipitation is enhanced in this zone because silica solubility is considerably reduced in areas with very small negative radii of curvature (Iler, 1973)(fig. 3). Thus, precipitating silica rapidly fills the embayment between any silica particles that come into contact and cements them together.

This cementation model explains the sediment-like

layering and the various textures of the sinter deposit. Under high flow rates or turbulance, such as near the vent, most suspended particles are swept off of the sinter surface before they can adhere. However, the few particles that do stick to the sinter become heavily overgrown by silica precititating directly from solution to produce a deposit of dense, vitreous sinter. Thus, the sinter near the springs and geysers is hard and dense. On the other hand, under low water velocities many more suspended particles can accumulate on the sinter surface and each layer of particles is covered by a successive one before they have been thoroughly cemented together. Thus, a more porous, chalky sinter is formed at a distance from the vents.

TOTAL DISCHARGE OF THE BEOWAWE SYSTEM

The total discharge of the Beowawe system over time can be estimated from the mass of the sinter deposit and the amount of silica deposited per kilogram of solution (P, see fig. 6) using the following equation:

$$D = M/P$$

==========

Figure 6.--near here.

==========

The bulk density of the sinter is estimated to be 1.66 g cm^{-2} and the total volume of the sinter deposit is estimated as 7.7×10^{13} cm^3; thus, the mass of the sinter deposit is about 1.28×10^{14} g. P is the difference between the

solubility of quartz at the reservoir temperature and that of amorphous silica at 25°C. If the reservoir temperature were 230°C throughout the life of the system, about 5.58×10^{14} kg of water would have been required to produce the Beowawe sinter deposit. It is possible that in the past the reservoir temperature of the Beowawe system was higher so the discharging water would have produced more sinter per unit mass. Assuming a reservoir temperature of 300°C as a reasonable maximum, the minimum amount of water necessary to produce this sinter deposit is around 2.66×10^{14} kg.

The size of the sinter deposit can also be used to estimate the total amount of heat carried to the surface by the geothermal waters. This can be done because both the amount of heat and the amount of silica brought to the surface per unit mass of water are a function of the reservoir temperature. Thus, the total amount of heat transported to the surface (H) over the life of the system can be found from:

$$H = M(\Delta H/P)$$

The enthalpy difference (ΔH) between pure water at saturation pressure and the temperature of the reservoir and the enthalpy of water at 25°C was calculated from Keenan, et al. (1978). The ratio of $\Delta H/P$ has been calculated for a range of temperatures and is displayed in figure 6. If the resrvoir temperature were 230°C the total heat production was 4.95×10^{17} kJ. On the other hand, if the reservoir

temperature were 300°C the heat production was 3.30×10^{17} kJ. Thus, the total amount of heat brought to the surface by the geothermal fluid that produced the Beowawe sinter deposit is around 4×10^{17} kJ. Around 1.2 kJ g^{-1}, of heat is released by cooling a basaltic intrusion from its liquidus temperature to 250°C (Norton and Cathles, 1979). Based on this, the minimum size of a basaltic intrusion that could be responsible for furnishing the heat to produce the Beowawe sinter deposit is 3.3×10^{17} g (115 km^3).

CONCLUSIONS

The sinter mound at Beowawe has many features similar to those found in sedimentary rocks. First, it shows bedding on a scale of tens of centimeters that is similar to sedimentary bedding. On a smaller scale it shows partings similar to those in shales. Finally, on a millimeter scale are fine bands. When the orientation of these features is observed in map scale a delta pattern emerges. It is likely that the sinter deposition was initiated at numerous points along the base of the Malpais Fault scarp and that the resulting sinter mounds coalesced to form a continuous deposit. These nearly flat-lying beds (dips less than 10°) are analogous to the topset beds of a delta. After these original outlets became choked with sinter, new conduits were formed by water flowing laterally through the sinter pile to discharge along its flanks. This activty on the flanks of the deposit produced the most steeply dipping (10-20°) layering that is dipping away from the source area

similar to foreset beds. Although geothermal sources may have occured further out in the valley their contribution to the sinter mass was apparently negligable compared with the amount of sinter deposited from the fluids produced through the Malpais fault trace. The beds in this area show low dips with no particular orientation and may be compared to bottomset beds. At the present time, fumarole and hot spring activity is almost exclusively restricted to the top and southwest end of the terrace.

The mechanism of formation of the siliceous sinter in the Beowawe deposit involves three steps. First, geothermal solutions that are saturated with quartz in the reservoir move to the surface and cool. When the solutions have cooled to a critical temperature amorphous silica nucleates. This nucleation is catalyzed by other suspended solids in the geothermal water, particularly amorphous ferric hydroxides. Finally, the particles of amorphous silica are agglomerated and attached to the sinter surface. This is a result of the rapid precipitation of silica around the contact point between two particles so as to minimize the surface free energy of the system. This mechanism is probably also responsible for the formation of siliceous scale in geothermal power systems.

The size and bulk density of the Beowawe deposit can be used to estimate that the amount of water discharged by the system was around 5×10^{14} kg. Furthermore, this water carried about 4×10^{17} kJ of heat to the surface. Although

the actual heat source is unknown, if the heat were furnished by a cooling basaltic intrusion, it would have to contain at least 115 km^3 of basalt to supply enough heat to account for the size of the Beowawe sinter deposit.

ACKNOWLEDGEMENTS

D.R.C. would like to thank M. Bullett for his assistance in field sampling. Chemical analyses of the hot spring and sinter samples were performed by Ruth Kroneman, Keith Yorgason, Bev Miller, and Frank Bakke. Funding for D.R.C. was provided by the U.S. Dept. of Energy, Division of Geothermal Energy under contract number DE-AC07-80ID12079. J.D.R. would like to thank Anthonio Lasaga for some very helpful comments on the nature of heterogeneous and homogeneous nucleation.

REFERENCES

Alexander, G. B., 1957, The effect of particle size on the solubility of amorphous silica in water: J. Phys. Chem., v. 61, p. 1563-1564.

Cosner, S. R. and Apps, J. A. (1978) Compilation of data on fluids from geothermal resources in the United States: University of California, Lawrence Berkeley Laboratory Report - 5936.

Fournier, R. O., and Rowe, J. J., 1966, Estimation of underground temperatures from the silica content of water from hot springs and wet-steam wells: Am. Jour. Sci., v. 264, p. 685-697.

Iler, R. K., 1973, Colloidal silica, in Matijevic', E. ed., Surface and Colloidal Science: v. 6, p. 1-100.

Iovenitti, J. (1981) Beowawe geothermal area evaluation program: Open-file Report to the Dept. of Energy by Cheveron Resources Co. under contract DOE/ET/27101-1.

Keenan, J. H., Keyes, F. G., Hill, P. G., and Moore, J. G., 1978, Steam Tables, Thermodynamic Properties of Water, Including Vapor, Liquid, and Solid Phases (International System of Units--S.I.): New York, John Wiley, 156 p.

Makrides, A. C., Turner, M, and Slaughter, J., 1980, Condensation of silica from supersaturated silicic acid solutions: J. Colloid Interface Science, v. 73, p. 345-367.

Nielsen, A. E., 1964, Kinetics of Precipitation: New York, Macmillan, 151 p.

Nielsen, A. E., and Sohnel, O., 1971, Interfacial tensions electrolyte crystal-aqueous solution, from nucleation data: J. Crystal Growth, v. 11, p. 233-242.

Norton, D., and Cathles, L. M., 1979, Thermal aspects of ore deposition, in H. L. Barnes, ed., Geochemistry of Hydrothermal Ore Deposits: New York, John Wiley, p. 611-631.

Nolan, T. B., and Anderson, G. H., 1934, The geyser area near Beowawe, Eureka County, Nevada: Am. Jour. Sci., v. 27, 215-229.

Renner, J. L., White, D. E., and Williams, D. L., 1975, Hydrothermal Convection Systems, in Assessment of Geothermal Resources of the United States--1975: U.S. Geological Survey Circular 726, p. 5-57.

Robie, R. A., Hemmingway, B. S., and Fisher, J. R., 1978, Thermodynamic properties of minerals and related substances at 298.15 K and 1 bar (10^5 Pascals) pressure and at higher temperatures: U.S. Geological Survey Bull. 1452, 456 p.

Rimstidt, J. D., and Barnes, H. L., 1980, The kinetics of silica-water reactions: Geochim. Cosmochim. Acta, v. 44, p. 1683-1699.

Rinehart, J. S., 1968, Geyser activity near Beowawe, Eureka, County, Nevada: J. Geophys. Res., v. 73, p. 7703-7706.

Rothbaum, H. P., Anderton, B. H., Harrison, R. F., Rhode, A. G., and Slatter, A., 1979, Effect of silica polymerization and pH on geothermal scaling: Geothermics, v. 8, p. 1-20.

Struhsacker, E. M., 1980, The geology of the Beowawe Geothermal System, Eureka and Lander Counties, Nevada: University of Utah Research Institute Report ESL-37 (DOE/ID/12079-7).

Zobak, M. L., 1979, A geologic and geophysical investigation of the Beowawe geothermal area, north-central Nevada: Stanford University Publications, Geological Sciences, v. 16, 79 p.

Uhlmann, D. R., and Chalmers, B., 1966, The energetics of nucleation in Nucleation Phenomena: Washington D.C., American Chemical Society, p. 1-13.

TABLE 1
The chemical composition of fluids and sinter from the Beowawe area

	(1)	(2)	(3)	(4)	(5)	(6)	(7)	(8)
	Hot Sp.	Hot Sp.	Hot Sp.	Well	Well	Sinter	Sinter	Sinter
T, °C	89	89	95	132	160			
T, °C(9)	192	186	203	217	240			
pH (10)	8.65	8.45	8.55	9.3	9.17			
Na(ppm)	219	206	204	214	277	2841	4948	3672
K (ppm)	18	14	24	9	35	1229	7297	2059
Ca(ppm)	12	1	1	13	2.5	2258	2287	2516
Mg(ppm)	1	<0.5	<0.5		0.3	289	772	326
Fe(ppm)	0.66	<0.025	<0.025		0.53	668	11193	1337
Al(ppm)	<0.625	<0.625	<0.625	0.2	1.1	1276	29059	3287
Ti(ppm)	<0.125	<0.125	<0.125			54	1906	138
P (ppm)	<0.625	<0.625	<0.625			22	271	26
Sr(ppm)	0.03	0.04	0.03			82	181	108
Ba(ppm)	0.63	<0.625	<0.625			27	645	54
Mn(ppm)	<0.25	<0.25	<0.25			23	85	31
W (ppm)	0.2	0.13	<0.125			<1200	<1200	<1200
As(ppm)	<0.625	<0.625	<0.625		<0.625	<25	<25	<25
Hg(ppb)						50	4395	137
Li(ppm)	1.52	1.43	1.50		1.94	13	34	13
Be(ppm)	<0.005	<0.005	<0.005			3.6	3.4	5.4
B (ppm)	2.0	1.8	1.9	1.0	2.0	<400	<400	<400
SiO_2(ppm)	236	218	274	329	436			
HCO_3(ppm)	345	340	159	33	175			
CO_3(ppm)			196	246	92			
SO_4(ppm)	99	92	107	89	76			
Cl (ppm)	31	19	36	50	67			
F (ppm)	18	22	15	6	12.2			
TDS(ppm)	958	898	1000	989	1240			

Notes: (Table 1)

(1) Hot spring sampled 12-3-81, location 1 in Figure 2.

(2) Hot spring sampled 12-3-81, location 2 in Figure 2.

(3) Boiling hot spring sampled 12-3-81, location 3 in Figure 2.

(4) Vulcan well - 2, analyses given by Cosner and Apps (1978), see Figure 2 for map location.

(5) Chevron well 85-18, analyses given by Iovenitti (1981(, see Figure 2 for map location, well depth is 1804m (5920 feet)

(6) Siliceous sinter sampled 12-3-81, location A in Figure 2.

(7) Siliceous sinter (massive) sampled 12-3-81, location B in Figure 2.

(8) Siliceous sinter (fissil) sampled 12-3-81 location B in Figure 2.

(9) Temperature calculated from the silica geothermometer (Fournier and Rowe, 1966).

(10) pH of the hot springs measured at temperature of spring, for wells, pH measured at ∿20°C.

FIGURE CAPTIONS

Fig. 1. Quartz and amorphous silica solubility as a function of temperature. A geothermal solution in equilibrium with quartz at 238°C will become supersaturated with amorphous silica when it is cooled to less than 100°C.

Fig. 2. Map of the Beowawe sinter deposit.

Fig. 3. Amorphous silica solubility at 25°C as a function of the radius of curvature of the particles. For particles with a positive radius of less than 0.05 micrometers the solubility is noticably greater than the bulk solubility. If the negative radius of curvature is less than 0.05 micrometers in the embayment between two particles, the solubility is less than the bulk solubility and the rate of silica precipitation will be accelerated in this zone. This causes the particles to be cemented together. (Diagram modified from Iler, 1973)

Fig. 4. The free energy of formation of a nucleus as it grows from a single molecule through the critical size (r*) to become a stable particle. Note that the free energy barrier is smaller in the case of heterogeneous nucleation because the effective surface free energy term in equation 1 is smaller.

Fig. 5. The flux of aqueous silica (J) (both polymers and monomers) onto solid silica particles forming in the solution as a function of temperature for a solution containing 345 ppm dissolved silica. The curves on the left illustrate homogeneous nucleation while those on the right are for heterogeneous nucleation of amorphous silica where the effective surface free energy is 10 and 20 ergs cm^{-2}.

Fig. 6. The amount of amorphous silica (P) that can precipitate from a geothermal solution cooled to 25°C as a function of the reservoir temperature. The solubility of amorphous silica at 25°C is 116 ppm and the solubility of quartz was calculated from the temperature functions reported in Rimstidt and Barnes (1980). Also, the amount of heat brought to the surface by the geothermal solution per gram of silica that it deposits ($_{\Delta}H/P$) as a function of the reservoir temperature. The enthalpy difference between the water in the reservoir at saturation pressure and 25°C was calculated from the values given in Keenan, et al. (1978).

Fig 1

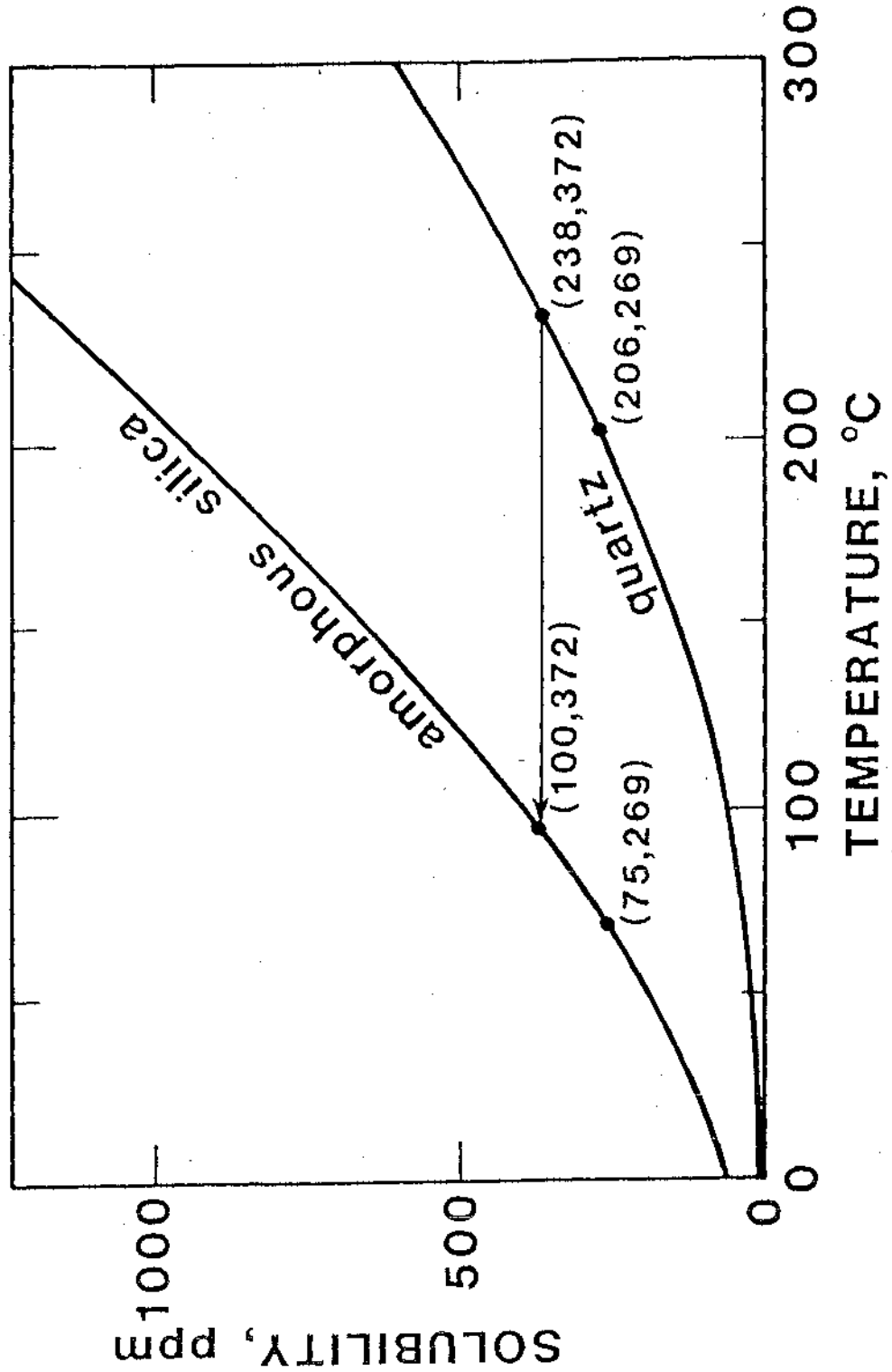
SOLUBILITY, ppm
1000
500
0
0
100
200
300
TEMPERATURE, °C
amorphous silica
quartz
(238,372)
(206,269)
(100,372)
(75,269)

Fig 2

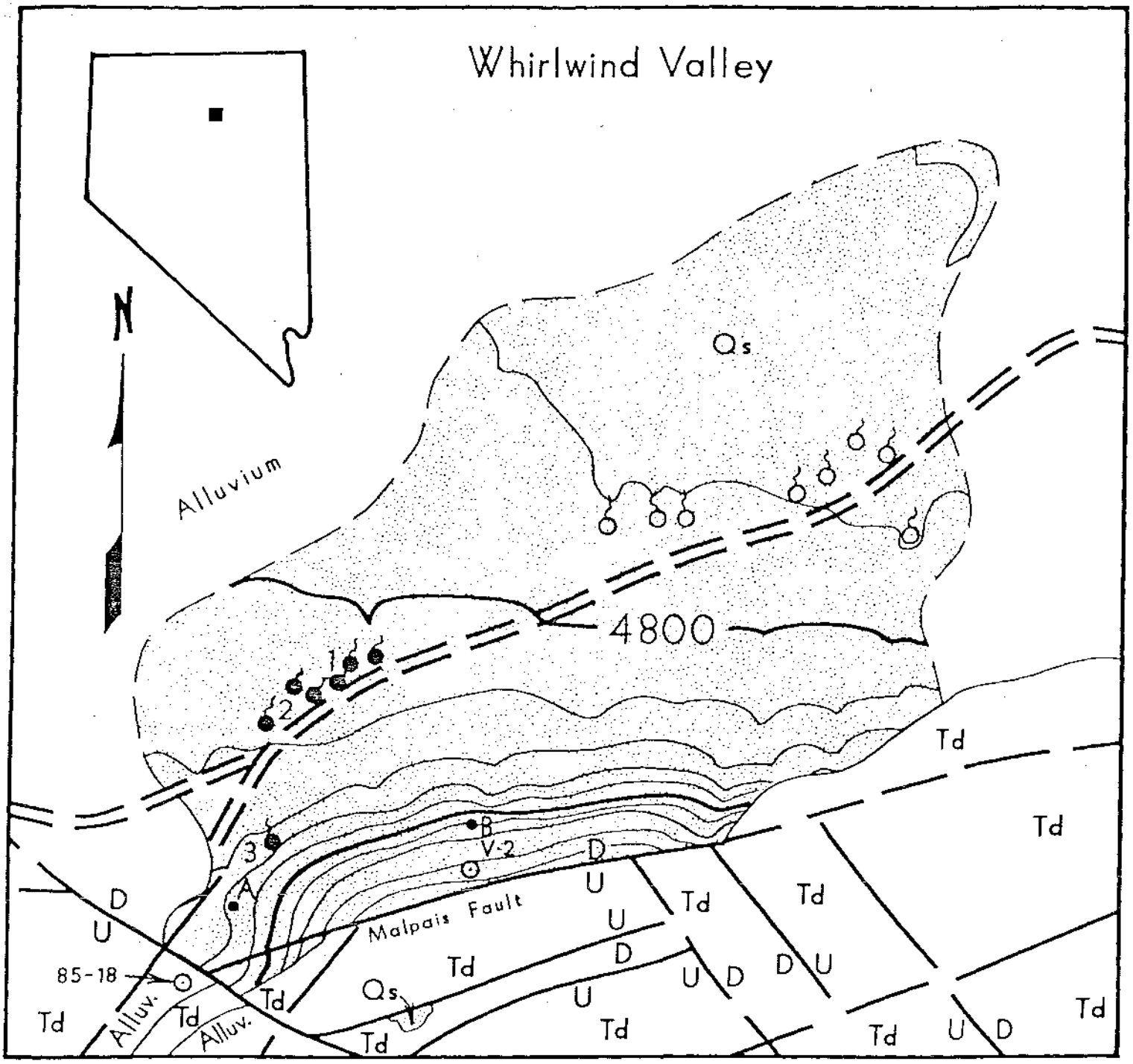
Whirlwind Valley
N
Alluvium
Qs
4800
1
2
3
A
B
V-2
D
U
Malpais Fault
85-18
Alluv.
Td
Qs
Contour interval : 40 ft.
0 1000 2000 3000 4000 5000 FEET
0 500 1000 METERS
Active hot springs
Extinct hot springs
Geothermal well
Road
A Sinter Sample Location
Qs Siliceous Sinter (stipled)
Td Tertiary pyroxene dacite
Normal fault, dashed where located approximately
Contact, dashed where located

Fig 3

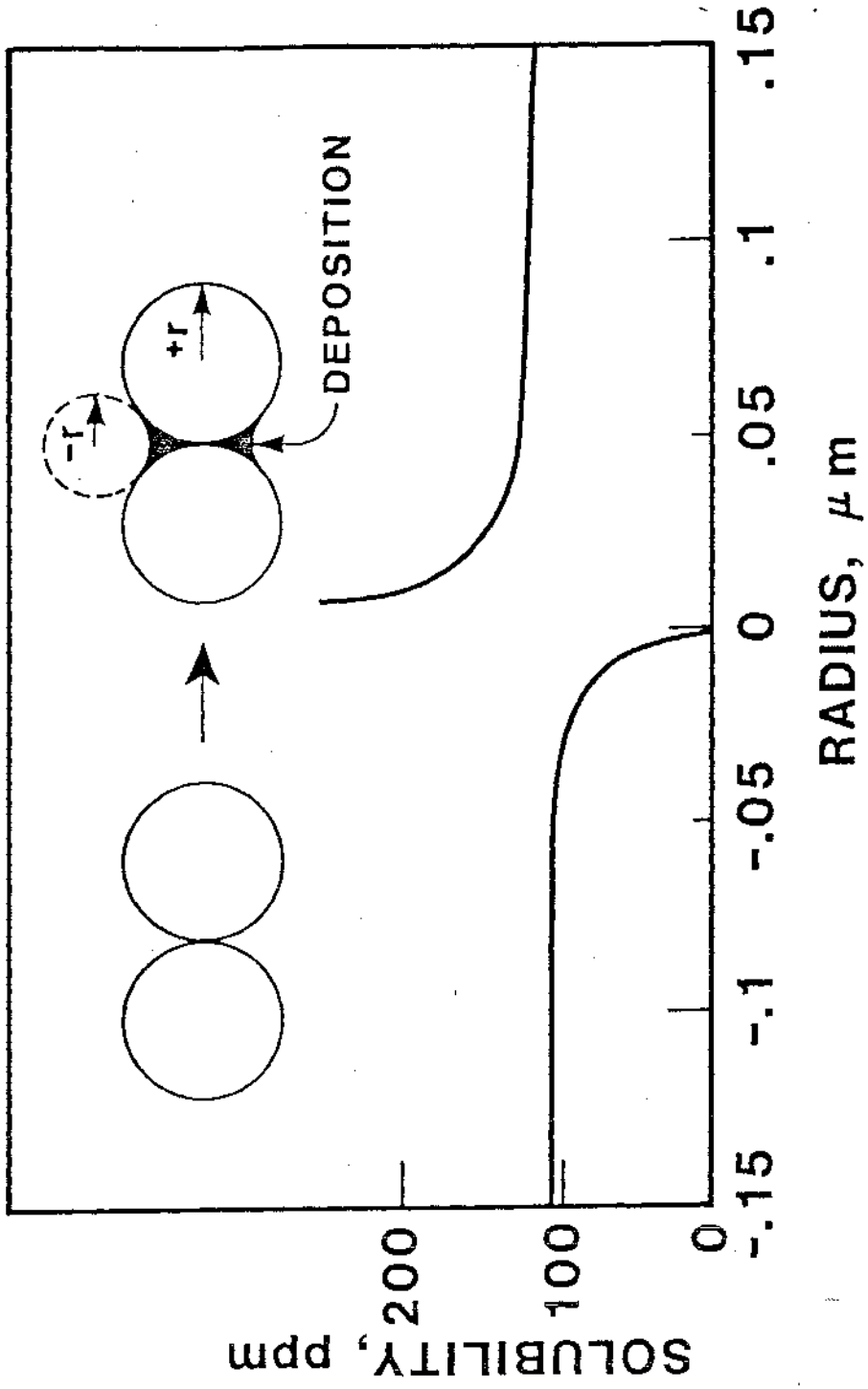
DEPOSITION
+r
-r
SOLUBILITY, ppm
200
100
0
-.15
-.1
-.05
0
.05
.1
.15
RADIUS, μm

Fig 4

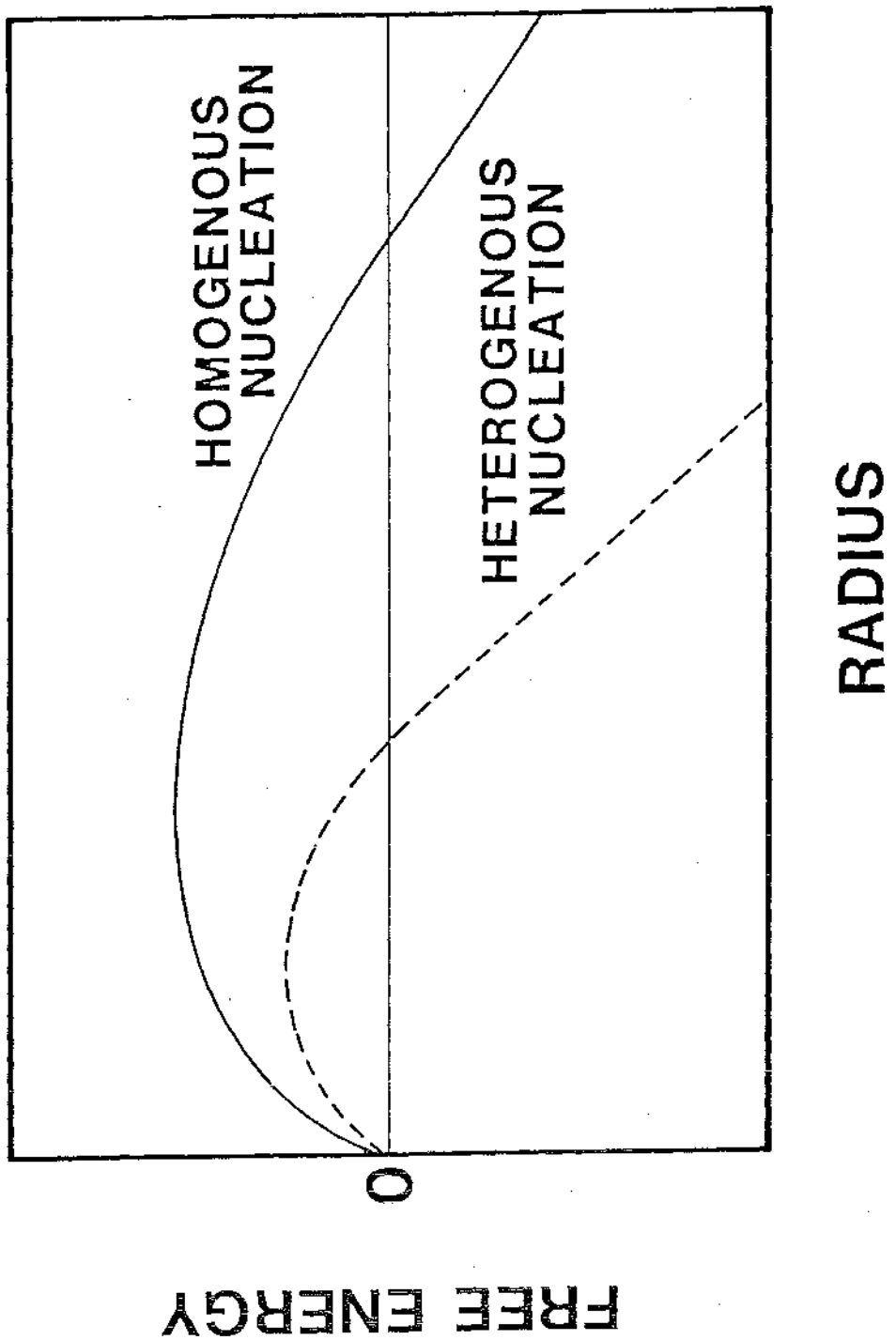
HOMOGENOUS NUCLEATION
HETEROGENOUS NUCLEATION
0
FREE ENERGY
RADIUS

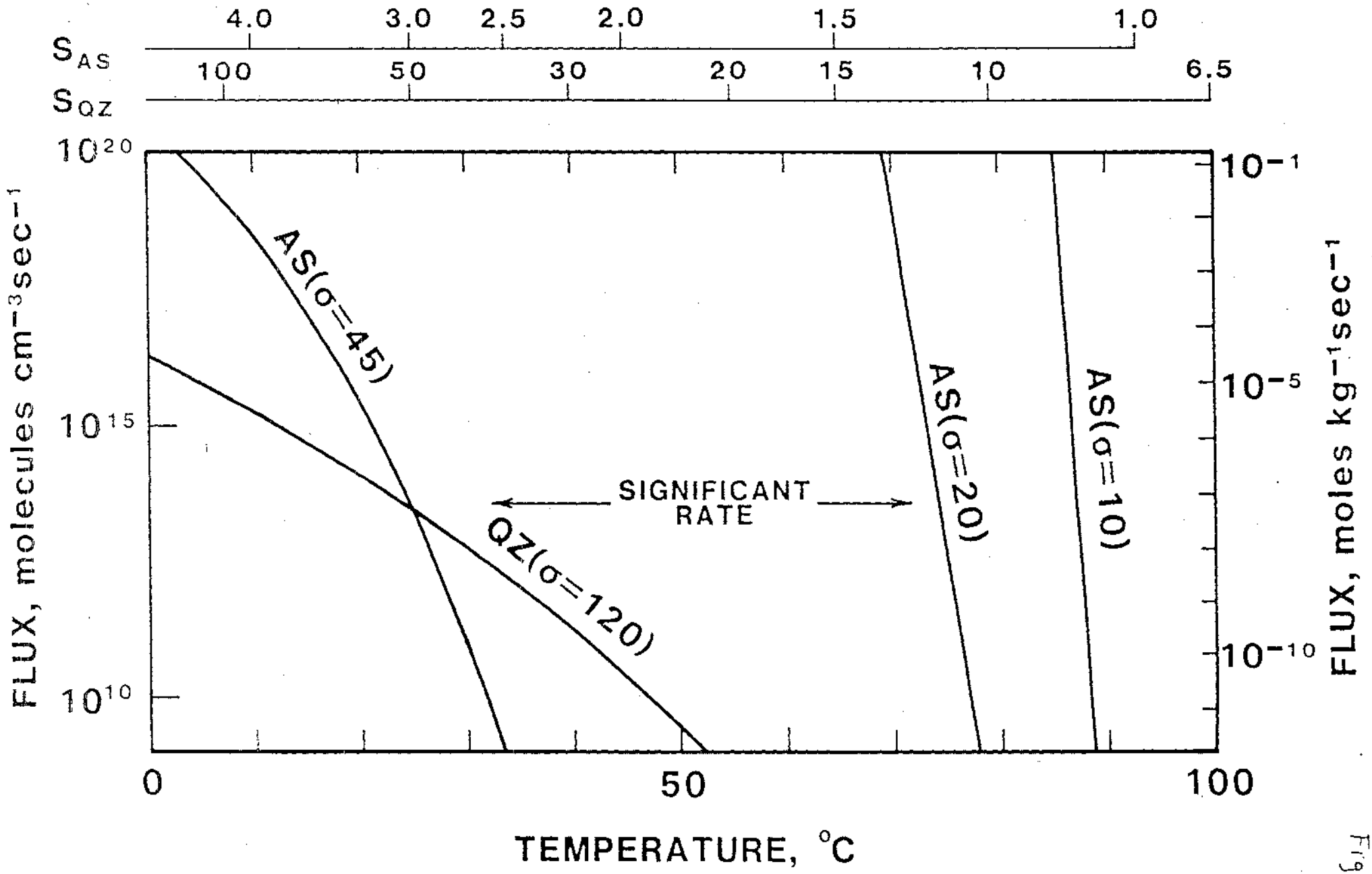
4.0
3.0
2.5
2.0
1.5
1.0
S_{AS}
100
50
30
20
15
10
6.5
S_{QZ}
10^{20}
10^{15}
10^{10}
FLUX, molecules $cm^{-3}sec^{-1}$
AS(σ=45)
QZ(σ=120)
SIGNIFICANT RATE
AS(σ=20)
AS(σ=10)
10^{-1}
10^{-5}
10^{-10}
FLUX, moles $kg^{-1}sec^{-1}$
0
50
100
TEMPERATURE, °C

Fig 5

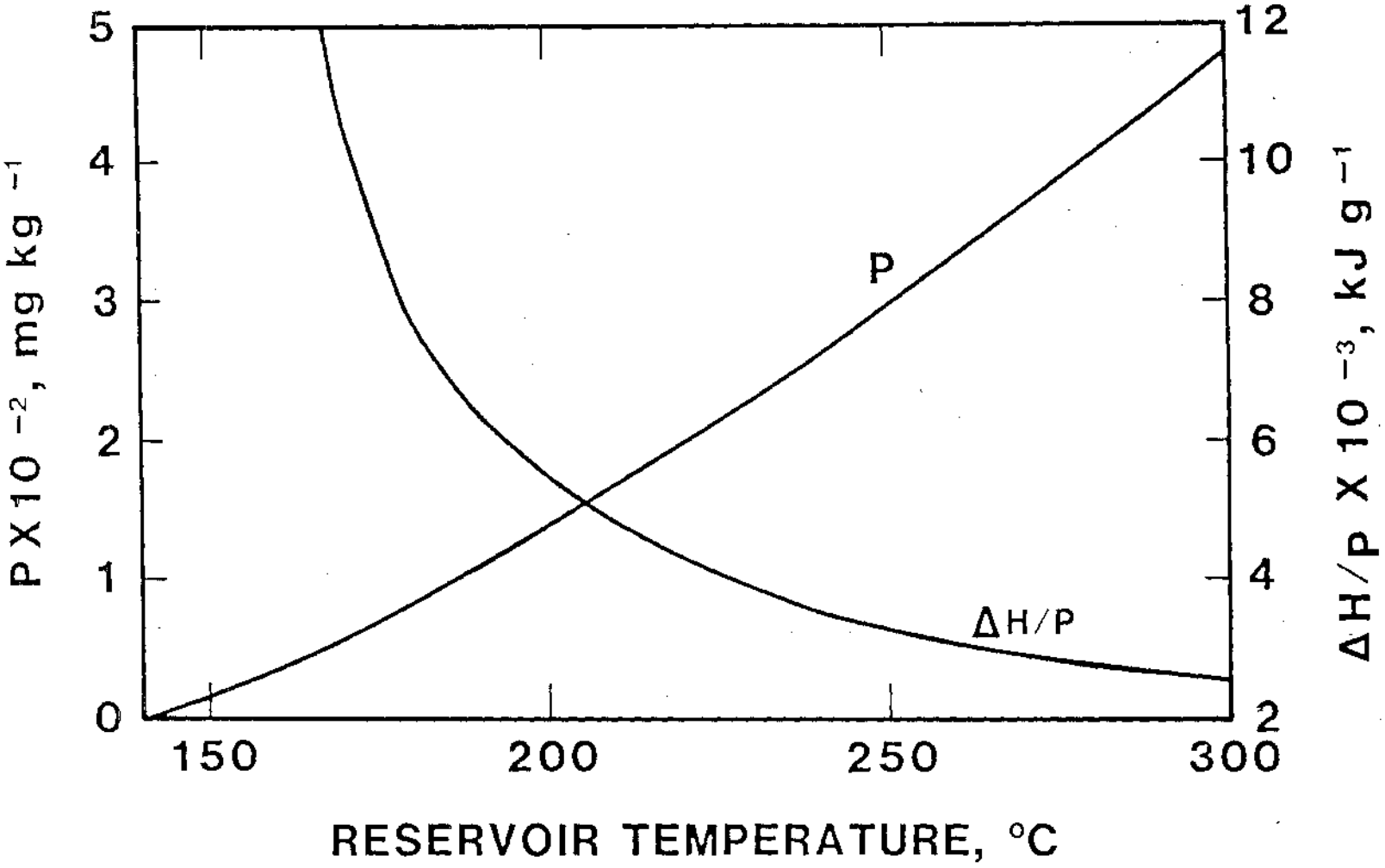
P X10 $^{-2}$, mg kg $^{-1}$
ΔH/P X 10 $^{-3}$, kJ g $^{-1}$
P
ΔH/P
0
1
2
3
4
5
2
4
6
8
10
12
150
200
250
300
RESERVOIR TEMPERATURE, °C